NUMERICAL MODELING OF NUCLEATION BOILING IN THIN FILM AND EFFECT OF DROPLET IMPACT

R. Panneer Selvam
BELL 4190 University of Arkansas
Fayetteville, AR 72701
Ph: 479-575-5356, email: rps@engr.uark.edu

R. Ponnappan
Air Force Research Laboratory, Propuslion Directorate
Wright-Patterson AFB, OH 45433-7251
Ph: 937-255-2922, email: rengasamy.Ponnappan@wpafb.af.mil

ABSTRACT

Recently it is identified that computer modeling of nucleation boiling in thin film of thickness in the order of 70 μm will provide valuable information in the design of experiments for spray cooling. Further work on computer modeling of vapor bubble growth in thin film of liquid considering both vapor and liquid in the computational region and preliminary work on the effect of droplet impact on thin liquid film is reported. The modifications to the incompressible Navier-Stokes equation to consider surface tension are detailed. The free surface movement is modeled using level set method. The detail of the phase change process using the level set method is described. The governing equations are solved using the finite difference method. The computed heat transfer during vapor bubble growth in thin film and impact of liquid droplet on thin film is reported. The flow pattern and temperature distribution at different times are graphically presented.

INTRODUCTION

Spray cooling is a high flux heat removal technique considered for high power systems such as advanced lasers. The spray cooling with phase change and droplet impact can achieve heat fluxes up to 1000 W/cm^2 as reported by Yang et al.[1]. Several experiments have been conducted using spray cooling in recent years[2-4] and various designs of spray cooling devices are emerging. Theoretical understanding of the spray cooling heat acquisition phenomena is still in its infancy and a focused effort to develop a comprehensive numerical model is a prime importance to this field.

Recently Selvam[5] and Selvam et al.[6] identified that computer modeling of nucleation boiling in thin film in the neighborhood of 70 μm will provide valuable information in the design of experiments for spray cooling. A survey on current status of computational modeling of spray cooling is presented. Details of methods to solve multiphase flow are reported. Preliminary computation of a growing of vapor bubble in thin film of liquid and the transient heat transfer on the wall are reported. They identified that high heat transfer takes place during the impact of liquid droplet on thin liquid film where vapor bubble is growing. Further work on computer

modeling of vapor bubble growth in thin film of liquid is reported here. This work considers both vapor and liquid in the computational region. Selvam et al. [6] concluded from their study that when the vapor bubble grows on a hot wall, the heat transfer from the wall gets reduced. The vapor bubble growth and movement from the wall are investigated to see the effect on heat transfer rate. Preliminary results on the effect of droplet impact on thin liquid film with growing vapor bubble are presented.

NUMERICAL FORMULATION FOR MULTIPHASE FLOW USING LEVEL SET METHOD

For a survey on numerical techniques used to model multiphase flow and their advantages and disadvantages one can refer to the literature [5-7]. Here, for computer modeling of liquid and vapor during nucleate boiling, the level set method introduced by Sussman et al.[8] for bubble dynamics which was modified by Son and Dhir[9] to accommodate the effect of phase change is used. The interface separating the two phases is captured by a function φ which is defined as a positive or negative distance from the interface. Similar to Son and Dhir[9] and Son et al.[10] the negative sign is chosen for the vapor phase and the positive sign is chosen for the liquid phase. For more details on the level set method and it application one can refer to Sethian[11] and Osher and Fedikw[12]. The extensive application of the level set method in various areas of science and engineering are illustrated with their basic development in the above two books.

GOVERNING EQUATIONS

In this model, the fluid properties including density, viscosity and thermal conductivity are constant in each phase and the flow is assumed to be incompressible. The Navier- Stokes equations considering the effect of surface tension, gravity and phase change at the interface are as follows:

$$\rho(\partial_t \mathbf{u} +\mathbf{u}. \nabla \mathbf{u}) = -\nabla p+ \rho\mathbf{g}- \sigma\kappa\nabla H + \nabla.\mu\nabla \mathbf{u} + \nabla.\mu\nabla \mathbf{u}^T \qquad (1)$$

$$\rho c_{pl}(\partial_t T +\mathbf{u}. \nabla T) = \nabla.k\nabla T \quad \text{for H>0} \qquad (2)$$

$$T=T_{sat} (p_v) \text{ for } H = 0$$

$$\nabla. \mathbf{u} = \mathbf{m} . \nabla\rho/ \rho^2 \qquad (3)$$

where : $\rho = \rho_v + (\rho_l- \rho_v)H.$ \qquad (4)

The value of μ and k are calculated using the similar relation in Eq. (4). Here:

$$H= 1 \text{ if } \varphi \geq 1.5 h \qquad (5)$$
$$= 0 \text{ if } \varphi \leq -1.5h$$
$$= 0.5+ \varphi/ (3h) + \sin[2\pi \varphi/(3h)]/(2\pi) \text{ if } |\varphi| \leq 1.5h$$

where h is a grid spacing. The Eq. (5) implies that the interface separating two phases is replaced by a transition region of finite thickness. The volume source term included in the continuity equation (3) due to liquid-vapor phase change is derived from the conditions of mass continuity and energy balance at the interface:

$$m = \rho(\mathbf{u}_{int}-\mathbf{u}) = k\nabla T/h_{fg} \tag{6}$$

In the level set formulation, the level set function φ, is advanced and reinitialized as:

$$\partial_t \varphi = - \mathbf{u}_{int} . \nabla \varphi \tag{7}$$

$$\partial_t \varphi = \varphi_o (1- |\nabla \varphi|) /\sqrt{(\varphi_o^2 + h^2)} \tag{8}$$

where φ_o is a solution of Eq. (7).

The surface tension effect is considered in the momentum equation by using a step function H (H=0 in the vapor and 1 in liquid) and κ is the interfacial curvature expressed as:

$$\kappa = \nabla . (\nabla \varphi/|\nabla \varphi|) \tag{9}$$
$$= (\varphi_y^2 \varphi_{xx} - 2 \varphi_y \varphi_y \varphi xy + \varphi_x^2 \varphi_{yy})/(\varphi_x^2 + \varphi_y^2)^{3/2} \text{ for 2D}$$

Here subscripts are differentiation with respect to φ. The surface tension force, $- \sigma\kappa\nabla H$ is implemented in the volume form to avoid the need for explicit description of the interface (Brackbill et al.[13]).

NONDIMENSIONAL FORM OF THE GOVERNING EQUATIONS

The nondimensional form of the above set of equations is derived using the characteristic length l_r, velocity u_r, time t_r and dimensionless temperature T^*. They are defined as follows:

$$l_r = \sqrt{\sigma/g(\rho_l- \rho_v)}, \ u_r = \sqrt{gl_r}, \ t_r = l_r / u_r \text{ and } T^* = (T-T_{sat})/(T_w-T_{sat}). \tag{10}$$

The reference values are taken in such a way that the gravity force becomes unity that is Froude number equal to 1 and the Weber number (We) is just above 1.0 if the density ratio of the liquid to vapor is larger. In addition, considering ρ, k, μ and c_p of liquid as reference values, the nondimensional equations without their superscripts are expressed as follows:

$$\rho(\partial_t \mathbf{u} +\mathbf{u}. \nabla \mathbf{u}) = -\nabla p+ \rho g_y - \kappa\nabla H/We + (\nabla.\mu\nabla \mathbf{u} + \nabla.\mu\nabla \mathbf{u}^T)/Re \tag{11}$$

$$\rho c_{pl}(\partial_t T +\mathbf{u}. \nabla T) = (\nabla.k\nabla T)/Pe \text{ for H>0} \tag{12}$$

$$\nabla. \mathbf{u} = Ja \ k \nabla T . \nabla\rho/ (Pe \ \rho^2) \tag{13}$$

$$\mathbf{u}_{int} = \mathbf{u} + Ja \, k \, \nabla T / (Pe \, \rho) \qquad\qquad (14)$$

where: $Re = \rho_l u_r l_r / \mu_l$, $We = \rho_l u_r^2 l_r / \sigma$, $Ja = c_{pl} \Delta T / h_{fg}$, $Pr = c_{pl} \mu_l / k_l$ and
$Pe = Re \, Pr = \rho_l u_r l_r c_{pl} / k_l$. Here g_y represents unit gravitational force in the y-direction. In the
equations 11 to 14, ρ, k, μ and c_p are dimensionless with respect to the reference values.

BOUNDARY CONDITIONS

The boundary conditions for the governing equations are shown in Figure 1 and also given
below:

At the wall (y=0): $u = v = 0$, $T = T_w$, $\varphi_y = 0$. At the planes of symmetry (x=0 and x= xmax): $u = v_x = T_x = \varphi_x = 0$. At the top of the computational domain (free surface, y= ymax): $u_y = v_y = \varphi_y = 0$, $T = T_{sat}$

y=ymax: $u_y = v_y = \varphi_y = 0$, $T = T_{sat}$
(free surface)

y

x=0
u= $v_x = 0$
$T_x = \varphi_x = 0$
(symmetry)

Staggered mesh

p

u,v, T, φ

x=xmax
u= $v_x = 0$
$T_x = \varphi_x = 0$
(symmetry)

x

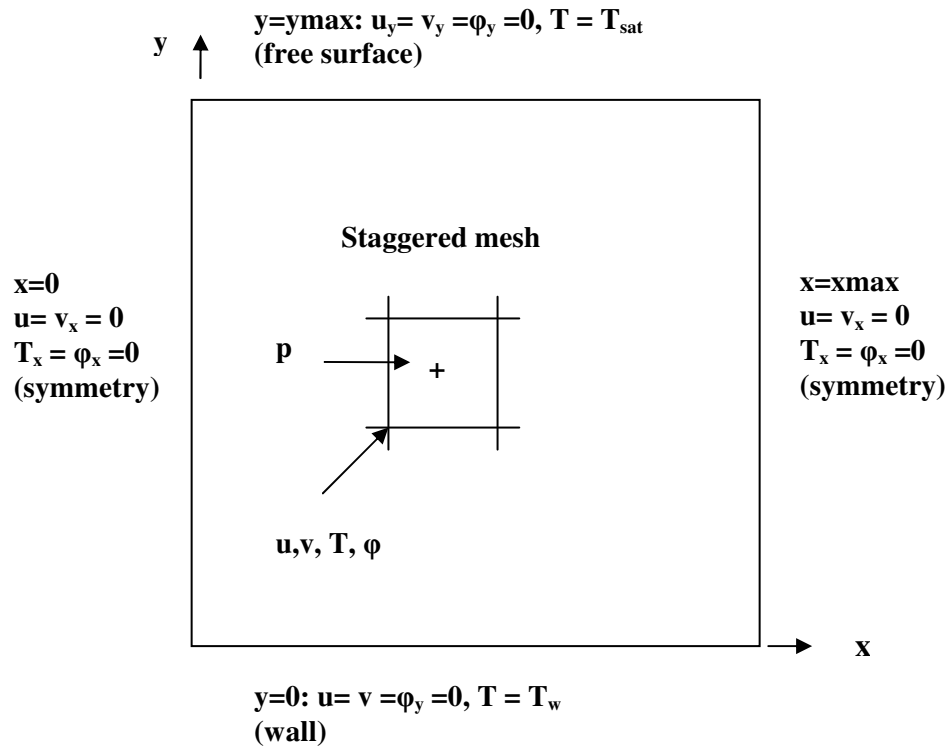**y=0: u= v =$\varphi_y = 0$, $T = T_w$**
(wall)

**Figure 1. Boundary conditions and the location of the variables stored in staggered grid
system**

NUMERICAL SOLUTION

The governing equations Eq. (1), (2), (3), (7) and (8) combined together are highly nonlinear.
The equations are discretized using finite difference method on a staggered grid system in which
all the variables except pressure are stored at the grid points; and pressure alone is stored at the

cell center as shown in Figure 1. The diffusion terms are considered implicitly and the convection and source terms are considered explicitly in time. For spatial approximations all terms are considered using second order central difference and the convection term by a second-order ENO method described by Chang et al. [14] to prevent numerical oscillations. The pressure and velocity are solved in a sequential manner by the procedure described in Selvam[15].

The discretized equations from the momentum, energy and pressure equations are symmetric and they are solved by the preconditioned conjugate gradient procedure (Ferziger and Peric[16]) in an iterative form. The iteration is done until the average residue for each node is reduced to less than 10^{-9}. This amount of accuracy is needed because of high density difference between liquid and vapor. After assuming initial position for distance functions, at each time step the equations are solved sequentially in the following order:

1. Solve the momentum equations, Eq. (1) for velocities
2. Correct the velocity to take the pressure effect
3. Solve the pressure Poisson equation to satisfy continuity
4. Update the velocities to include the new pressure effect
5. Solve temperature equation Eq. (2)
6. Solve the distance function Eq. (7)
7. Reinitialize the distance function as per Eq. (8) and go to next time step

During the computation, time steps were chosen to satisfy the Courant-Fredreichs-Lewy (CFL) condition, $\Delta t \leq \min (h/(|u|+|v|), 10^{-6})$. This was done because of the explicit treatment of the convection terms and the condition that the numerical results should not change if the time steps are halved.

RESULTS AND DISCUSSION

Lin and Ponnappan[4] conducted spray cooling experiments using FC-72 for different T_{sat}. As an example $T_{sat} = 53\,^{\circ}$ C case is considered. For this temperature, the computed reference values are: reference length $l_r = 736.2$ μm, reference velocity $u_r = 85$ mm/s, reference time $t_r = 8.66$ ms and $\Delta T = 10\,^{\circ}$ C. The density ratio of liquid to vapor (ρ_l/ρ_v) is 138 and other nondimensional numbers are: Re= 218, We=1.0, Pe = 2050 and Ja =0.127. For initial study, the parameters considered are: $\rho_l/\rho_v = 20$, Re= 200, We=1.0, Pe = 1000 and Ja =0.1. Low density ratio is considered to reduce computer time and to avoid numerical instability. The computed results for higher density ratio has similar trend as low density ratio but the time step needs to be much smaller. Further study in the future will consider higher density ratios in detail.

Time steps considered are 5×10^{-6} (43.3 ns) and 1×10^{-6} (8.66 ns) nondimensional time. The computational domain considered are 0.1 units x 0.1 units which is equal to 73.62 μm x 73.62 μm. The computational domain is discretized by 51x51 and 101x101 mesh at this time. The 101x101 mesh is considered to compare the results from 51x51 mesh and to evaluate the convergence. Most of the runs are made using 51x51 mesh. The smallest grid size varied from 7.362 μm to 14.724 μm.

MODELING A BUBBLE AT A DISTANCE FROM THE WALL

In Selvam[5] and Selvam et al.[6] the whole computational domain is assumed to have liquid and the vapor bubble is assumed to grow at the origin. The initial bubble size is assumed to have a radius of 0.02 units which is about 10 grid points. The temperature is assumed to be T_{sat} everywhere except at the wall T= T_w to start and the model is allowed to run for 80,000 time step (692.8 μs) with a time step of $1.x10^{-6}$ (8.66 ns) nondimensional time. The average Nu decreases with time and at the end of the 692.8 μs the average of Nu at the wall was 50 and the radius of the vapor bubble was 0.034 units. When considering nucleate boiling in a thin liquid film of 73.62 μm in gravity; there is not much room for the vapor bubble to grow and depart into a pool of liquid. Son et al.[10] reported that the bubble diameter to be varying from 2.5 mm to 3 mm from both experiment and computer modeling. In a thin liquid film, there is not enough space for a vapor bubble to grow to its fullest extent. Before that happens, the bubble bursts and merges with vapor on the top of the liquid layer on its own or due to the impact of a spray droplet. Hence, the present modeling study carried out to show the increase in Nu when a small bubble is at a little distance away from the wall.

In the same computational domain of 0.1x0.1 dimensionless unit, a bubble with radius of 0.04 units is kept at 0.05 units from the wall as initial condition. Temperature is assumed to be T_{sat} everywhere except the wall to start and the model is allowed to run for 80,000 time steps (692.8 μs) with a time step of $1x10^{-6}$ (8.66 ns) nondimensional time. The final velocity vector diagram and temperature contour plot are plotted in Fig. 2.
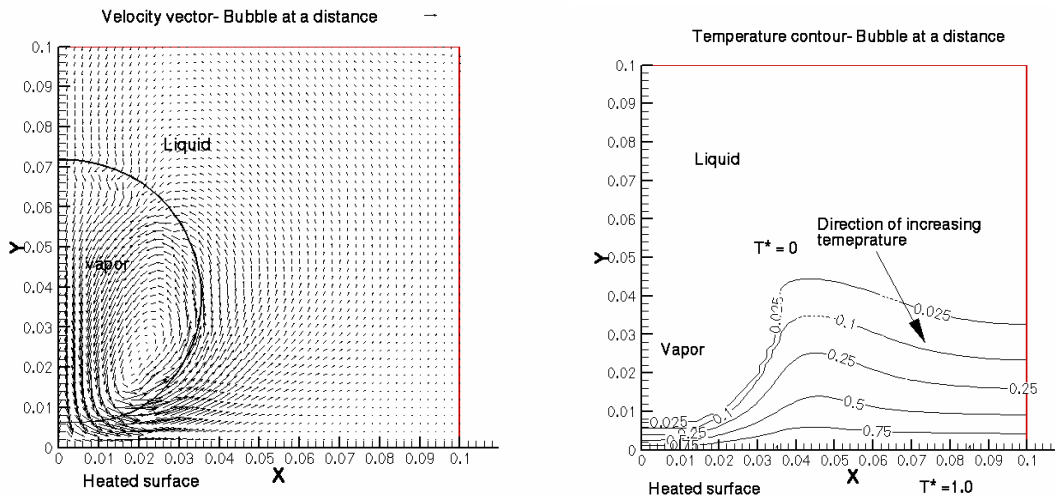

Figure 2. Veocity vector and temperature contour diagram for bubble in FC-72 at a distance from the wall after 692.8 μs.
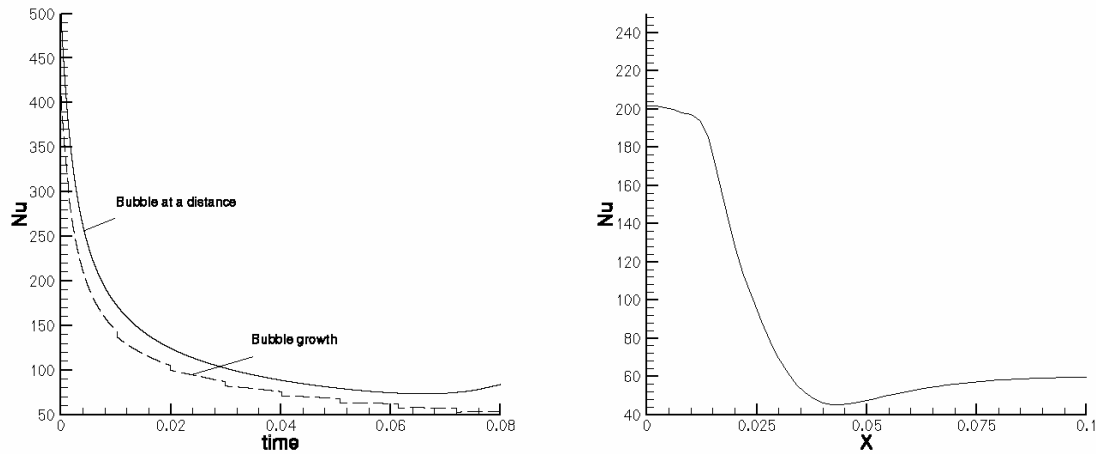
Figure 3. Variation of average Nusselt number over the hot surface with time for up to 692.8 μs and instantaneous Nusselt number along the hot surface at 0.08 dimensionless time (692.8 μs)

The bubble in Fig. 2 has a radius close to 0.035 units which is less than 0.04 units to start with. Initially it is assumed that the velocity in most of the domain is zero. Hence the flow evaluation in time with temperature to satisfy the governing equation could have caused this change. The temperature boundary layer propagates in time and the depth reached about 0.03 units on the far right as shown in Fig. 2. This depth is similar to bubble growth in Selvam et al.[6] at the same place. At the same time close to bubble one can see clearly a thin boundary layer of 0.006 units. The average Nu at the wall for the bubble growth case and bubble at a distance case are shown in Fig. 3. The average Nu decreases with time because in the initial stages when time t is small the q is very high due to transient conduction as explained in Selvam et al.[6]. Here one can see that the Nu for the bubble being at a distance from the wall is higher than the bubble growing on the wall case. When the bubble is away from the wall the minimum Nu is about 70 whereas for growing-bubble case it is 50. The Nu distribution along the wall at 0.08 units of time is also plotted in Fig. 3. The Nu is around 200 on the wall in the region below the bubble and in other areas it is around 50. So the bubble creates a thin thermal boundary layer. A similar trend is reported by Son et al.[10] when a bubble grows and departs. Collapsing the bubble by liquid droplet impact or moving the bubble from the nucleation site by other means only can bring cooler liquid close to the wall that can achieve higher Nu in the order of 200 as reported by Lin and Ponnappan[4].

MODELING A DROPLET IMPACT ON THIN LIQUID FILM

To study the impact of droplet on thin liquid film with vapor bubble growing, a vapor bubble with radius 0.055 (40.491 μm) units in a liquid layer of 0.06 (44.172 μm) units is considered as shown in Fig. 4. A droplet diameter of 0.06 units falling down with a speed of 30 (2.55 m/s) units located at 0.13 units from the hot wall is considered. The droplet is assumed to fall right over the vapor bubble growing. Other cases will be considered in future work. These parameters are close to the 40 μm diameter of spray falling with a velocity of 10m/s reported by Baysinger et al.[17]

from experiment. The frequency of the falling droplet is suggested to be 1KHz (1 ms interval) by Harris[18] from observation. The velocity of 2.55 m/s (30 units) considered in the numerical modeling is slightly lower than the 10m/s. Even for the velocity of 30 units during impact, the maximum velocity in the computational region as shown in Fig. 5 increases up to 70 units which is the limit of the computational domain at this time. Further calculations with higher velocity will be done in the future. Due to impact, the velocity and flow change considerably and hence a computational domain of 0.2x0.2 unit with 201x201 grid size is considered. Computation is done with a time step of $5.x10^{-6}$ (43.3 ns) for 4000 time steps.
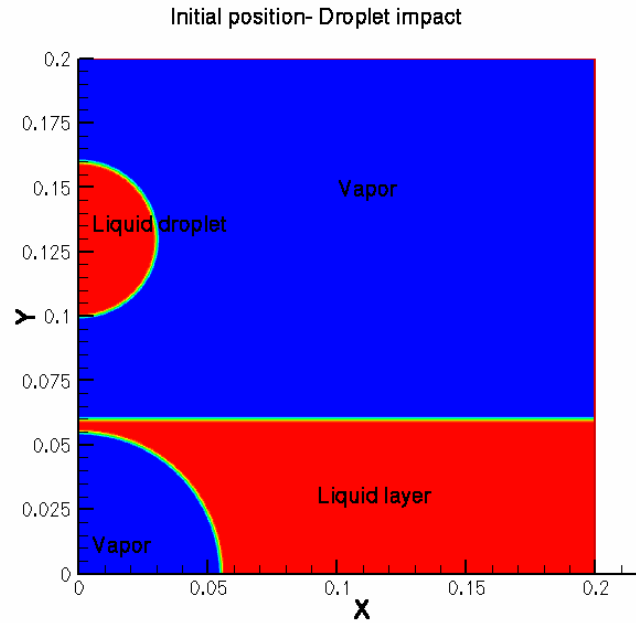

Figure 4. Computational region for droplet impact

The computed average Nu and the corresponding maximum velocity in the region with time are reported in Figure 5. The average Nu is decreasing consistently from 70 to 20 during the impact because the droplet could not break the bubble. The shape of the liquid and vapor layers before and after impact are presented in Figure 6. The corresponding average Nu and maximum velocity in the region for Figures 6(a) to 6(d) are (68.4, 57.3 units), (64.8, 31.44 units), (60.0, 30.1 units) and (11.4, 13.8 units) respectively. The maximum velocity in the region is around 70 as reported in Figure 5. This may be close to the situation of Fig. 6 (a). As the droplet falls down where the thickness of the liquid film is thin, the newly added liquid attaches to the liquid film and provides more strength to the film as shown in Fig. 6(b). Thus only the vapor evaporates at the bottom but the new liquid could not replace the old one. The Figure 6 illustrates how the liquid drop spreads outwards on the top of the liquid layer and compresses towards the wall. Other positions of droplet falling and its impact on heat removal will be reported in the future.
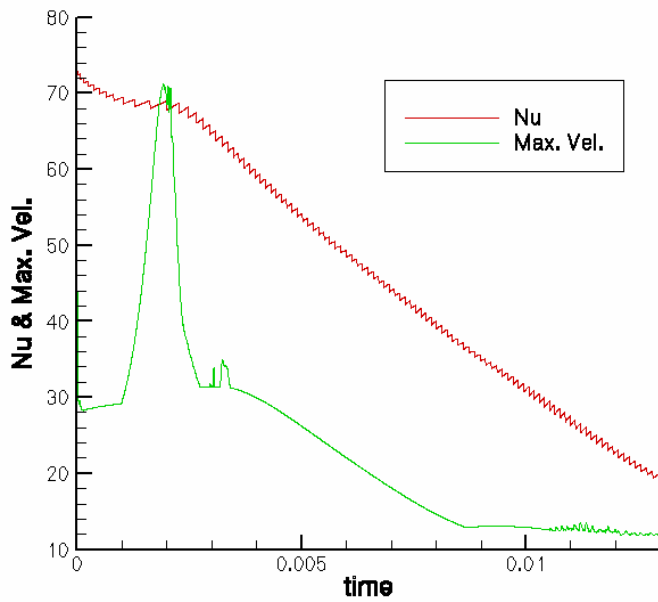
Figure 5. Variation of average Nusselt number over the hot surface and maximum velocity in the computational region with time up to 0.013 units (112.6µs).
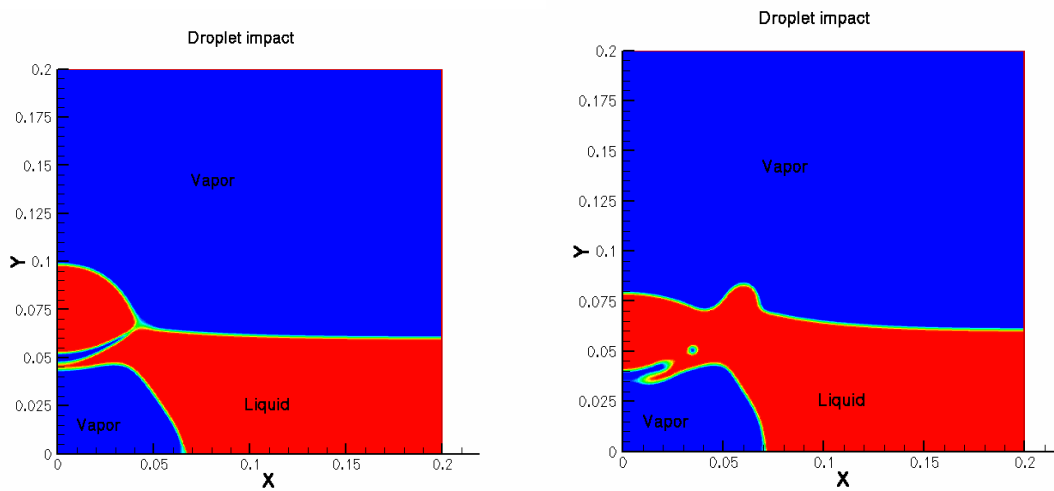

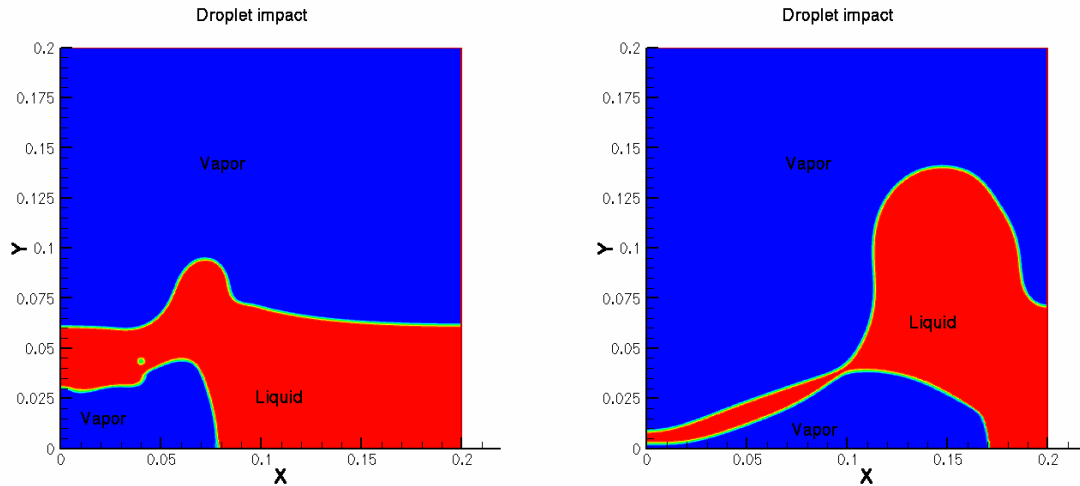**Fig.6 (a) 0.0022 units of time (b) 0.003 units of time**

Fig. 6 (c) 0.0039 units of time (d) 0.015 units of time
Figure 6. Shape of the liquid and vapor layer at different times during droplet impact

CONCLUSIONS

Numerical modeling of multiphase flow using level set method is discussed. The computer model is used to study the heat transfer mechanism in thin film of liquid with vapor bubble at a distance from the hot wall. From the study one can observe that when the vapor bubble is just above the wall can transport more heat than when the vapor is growing on the wall. Preliminary study on the impact of liquid droplet on a thin liquid film with vapor bubble growing is reported. In the present study, it is observed that the vapor bubble could not be broken with a low velocity directly hitting spray droplet. Further study of impacting the droplet at other locations around the vapor bubble and velocity effects are needed to understand the high heat transfer mechanism in the spray cooling.

ACKNOWLEDGEMENTS

REFERENCES

1. J. Yang, L.C. Chow and M.R. Paris, Nucleate boiling heat transfer in spray cooling, *Journal of Heat Transfer*, 118, 668-671, 1996

2. L.C. Chow, M.S. Sehembey and M.R. Paris (1997), High heat flux spray cooling, *Ann. Rev. Heat Transfer*, 8, 291-318

3. I. Mudawar (2001), Assessment of high heat-flux thermal management schemes, *IEEE Transactions on Components and Packaging Technologies*, 24, 122-141

4. L. Lin and R. Ponnappan, (2003), Heat transfer characteristics of spray cooling in a close loop, *Int. J. Heat Mass Transfer*, 46, 3737-3746

5. R.P. Selvam (2004), Numerical modeling of spray cooling phenomena for thermal management of high power systems, Report to Universal Technology Corporation, Dayton, OH, August

6. R.P. Selvam, L.Lin and R. Ponnappan (2005), Computational modeling of spray cooling: Current status and future challenges, Paper submitted to Space Technology and Applications International Forum (STAIF 2005), Conference on Thermophysics in Microgravity, Albuquerque, NM, Feb. 13-17

7. G. Trggvason et al. (2001), A front-tracking method for the computations of multiphase flow, *J. Comp. Physics*, 169, 708-759.

8. M. Sussman, P. Smereka and S. Osher, (1994), A level set approach for computing solutions to incompressible two-phase flow, *J. Comp. Physics*, 114,146-159

9. G. Son, and V.K. Dhir (1998), Numerical simulation of film boiling near critical pressures with a level set method, *Journal of Heat Transfer*, 120, 183-192.

10. G. Son, N. Ramanujapu and V.K. Dhir (2002), Numerical simulation of bubble merger process on a single nucleation site during pool nucleate boiling, *Journal of Heat Transfer*, 124, 51-62.

11. J.A. Sethian (1999), *Level set methods and fast marching methods: Evolving interfaces in computational geometry, fluid mechanics, computer vision and materials science*, Cambridge University Press, Cambridge, UK.

12. S. Osher and R. Fedkiw (2003), *Level set methods and dynamic implicit surfaces*, Springer, New York. Applies Mathematical Sciences: Vol. 153.

13. J.U. Brackbill, D.B. Kothe and C. Zamach (1992), A continuum method for modeling surface tension, *J. Comp. Physics*, 100, 335-354.

14. Y.C. Chang, T.Y. Hou, B. Merriman and S. Osher (1996), A level set formulation of Eulerian interface capturing methods for incompressible fluid flows, *J. Comp. Physics*, 124, 449-464.

15. R. P. Selvam (1997), Computation of pressures on Texas Tech building using large eddy simulation, *J. Wind Engineering and Industrial Aerodynamics*, 67 & 68, 647-657.

16. J.H. Ferziger and M. Peric (2002), *Computational Methods for Fluid Dynamics*, Springer, New York.

17. K.M. Baysinger et al. (2004), Design of a microgravity spray cooling experiment, *AIAA-2004-0966*, 42nd AIAA Aerospace Sciences Conference and Exhibit, Jan. 5-8, Reno, NV

18. R.J. Harris (2004), Private communications, University of Dayton Research Institute, Dayton, OH

CONTACT

Dr. R. Panneer Selvam is currently a Professor of Civil Engineering and Director of Computational Mechanics Laboratory at the University of Arkansas. He is currently involved in thermal management of high heat flux for power electronic devices and electronic packaging, multiphase flow modeling of spray cooling in micro and macro gravity environment, atomistic modeling of thermal effects on grain boundary of nanocrystals, multiscale (nano & continuum mechanics) modeling for material science and computer modeling tornado effects on buildings. He has been involved in computer modeling for engineering and science applications for the last 20 years. He has worked on computer modeling of bridge flutter, panel flutter, pollutant transport around buildings, thermal and creep stress analysis of electronic packaging and fracture mechanics. He has published more than 150 research papers. He is a member of ASCE, AAWE and IMAPS. Email: rps@engr.uark.edu, tel: 479-575-5356, fax: 479-575-7168.

Dr. Ponnappan is currently a Senior Mechanical Engineer and in-house Program Manager at Air Force Research Laboratory. He is actively involved in thermal management research and manages several AF funded programs including spray cooling and has made significant contributions in heat pipes and electronics cooling area. He has pursued thermal technologies for over 25 years; organized and chaired sessions in many technical conferences. He co-invented the concept of double-wall artery wick and explored gas-loaded liquid metal heat pipe startup and developed facilities at WPAFB for testing heat pipes in high 'g' centrifuge. His 'rotor cooling structure' patent has been licensed by an aircraft alternator manufacturer for improving bearing life and reliability. Dr. Ponnappan pioneered research on the high speed rotating heat pipe. He is author of five US patents and over a hundred research publications. He is an Associate Fellow of AIAA and Fellow of ASME-International. Email: rengasamy.ponnappan@wpafb.af.mil Tel: 937-255-2922; DSN: 785-2922; Fax: 937-904-7114.

NOMENCLATURE

c_p	specific heat at constant pressure
g	gravity vector
H	step function
h	grid spacing
h_{fg}	latent heat of evaporation
Ja	Jacob number = $c_{pl} \Delta T / h_{fg}$
k	thermal conductivity
l_r	characteristic length $\sqrt{\sigma / g(\rho_l - \rho_v)}$
m	mass flux vector
Nu	Nusselt number $q\, l_r / (\Delta T\, kl)$
p	pressure
Pe	Peclet number = $\rho_l u_r l_r c_{pl} / k_l$
Pr	Prandtl number = $c_{pl} \mu_l / k_l$

q	heat flux
Re	Reynolds number $= \rho_l u_r l_r / \mu_l$
T	temperature
T^*	dimensionless temperature $(T-T_{sat})/(T_w-T_{sat})$
ΔT	temperature difference $T_w - T_{sat}$
t	time
t_r	characteristic time l_r / u_r
u	velocity vector (u,v)
u$_{int}$	interface velocity vector
u_r	characteristic velocity $\sqrt{gl_r}$
We	Weber number $= \rho_l u_r^2 l_r / \sigma$
α	thermal diffusivity
κ	interfacial curvature
μ	dynamic viscosity
ρ	density
σ	surface tension
φ	level set function

SUBSCRIPTS

int	interface
l, v	liquid , vapor
sat, w	saturation, wall